Clays and Clay Minerals, Vol. 34, No. 2, 165–179, 1986.

TRANSMISSION AND ANALYTICAL ELECTRON MICROSCOPY OF THE SMECTITE-TO-ILLITE TRANSITION[1]

JUNG HO AHN AND DONALD R. PEACOR

Department of Geological Sciences, The University of Michigan
1006 C. C. Little Building, Ann Arbor, Michigan 48109

Abstract—The smectite to illite reaction was studied by transmission and analytical electron microscopy (TEM/AEM) in argillaceous sediments from depths of 1750, 2450, and 5500 m in a Gulf Coast well. Smectite was texturally characterized as having wavy 10- to 13-Å layers with a high density of edge-dislocations, and illite, as having relatively defect-free straight 10-Å layers. The structures of smectite and illite were not continuous parallel to (001) at smectite-illite interfaces. AEM data showed that the smectite and illite were chemically distinct although smectite had a more variable composition. Illite formation appeared to have initiated with the growth of small packets of illite layers within subparallel layers of smectite matrix. With increasing depth, ubiquitous thin packets of illite layers increased in size until they coalesced.

A model for the transition requires that the structure of smectite was largely disrupted at the illite-smectite interface and reconstituted as illite, with concomitant changes in the chemistry of octahedral and tetrahedral sites. At least partial Na-K exchange of smectite preceded illite formation. Transport of reactants (K, Al) and products (Na, Si, Fe, Mg, H_2O) through the surrounding smectite matrix may have taken place along dislocations.

The smectite-to-illite conversion process for the studied samples does not necessarily appear to have required mixed-layer illite/smectite as an intermediate phase, and TEM and AEM data from unexpanded samples were found to be incompatible with the existence of mixed-layer illite/smectite in specimens whose XRD patterns indicated its presence.

Key Words—Analytical electron microscopy, Burial diagenesis, Illite, Interstratification, Smectite, Transmission electron microscopy.

INTRODUCTION

General aspects of the smectite-to-illite reaction have been studied by many workers using argillaceous sediments from the Gulf Coast (Powers, 1967; Burst, 1969; Perry and Hower, 1970; Weaver and Beck, 1971; Hower *et al.*, 1976; Boles and Franks, 1979). These studies suggest a trend of increasing proportion of illite within mixed-layer illite/smectite (I/S) with increasing depth. Ordered I/S was described as characteristic of later stages of the reaction by Perry and Hower (1970), Weaver and Beck (1971), Hower *et al.* (1976), and Boles and Franks (1979), and reviews of reaction mechanisms were given by Środoń and Eberl (1984) and Eberl (1984).

The results of Hower *et al.* (1976) are central to the mechanism of the smectite-to-illite reaction. These authors investigated mineralogical and chemical changes in cores of Oligocene-Miocene argillaceous sediments from the Gulf Coast and proposed that the process can be approximated by the reaction:

$$\text{smectite} + Al^{+3} + K^{+} = \text{illite} + Si^{+4}.$$

This reaction implies that smectite transforms to illite directly by fixation of K in interlayer sites with a concomitant substitution of Al for tetrahedrally coordinated Si; i.e., the basic T-O-T atomic arrangement remains largely unchanged, and a 1:1 relationship exists between the relative number of parent smectite and the product illite layers.

Hower *et al.* (1976) concluded that these Gulf Coast shales behaved essentially as closed systems. K and Al were hypothesized to be supplied locally by the dissolution of K-feldspar (and/or mica), as evidenced by a concomitant decrease of K-feldspar and increase in the proportion of illite layers in I/S with depth. In addition, the data of Aronson and Hower (1976) showed that the whole-rock K-Ar age decreased within the interval where the fine clay fraction (<0.1 μm) gained radiogenic argon. These data support the interpretation that phases such as K-feldspar, mica, and discrete illite decomposed during burial diagenesis to supply K for the increasing proportion of illite layers of the I/S.

A different mechanism was proposed by Boles and Franks (1979); they hypothesized that the Al required for the formation of illite layers was derived from the smectite itself, not from an external source. They suggested that approximately 3 smectite layers transform to 2 illite layers, thereby implying that at least some of the original smectite layers must be destroyed. The Boles and Franks mechanism conflicts with that proposed by Hower *et al.* (1976) wherein all of the basic 2:1 structural units are retained. In addition, Eberl and

[1] Contribution No. 412, the Mineralogical Laboratory, Department of Geological Sciences, The University of Michigan, Ann Arbor, Michigan 48109.

Hower (1977), Eberl (1978a, 1978b), Lahann and Roberson (1980), and Roberson and Lahann (1981) experimentally brought about the conversion of smectite to I/S in the absence of an external source of Al, consistent with the mechanism proposed by Boles and Franks (1979).

Arguments for one or the other of these transformation mechanisms have generally been based on elemental and XRD analyses of separated clay fractions and only indirectly relate to individual smectite and illite layers. The chemical data, for example, were likely obtained on concentrations of clay-size material which may or may not have been monomineralic. Thus, the sample may have contained other phases, some of which may have been non-phyllosilicates (e.g., carbonates); some, however, may have been chlorite or kaolinite which may have played a direct role in the transformation. In the present study, a transmission and analytical electron microscopic (TEM/AEM) study of the smectite-to-illite transformation has been carried out. These methods are capable of providing high-resolution data on the texture, chemistry, and structure of specific portions of the individual phases involved in the reaction. The reaction mechanism described in this study on the basis of the TEM/AEM data differs from those of both Hower *et al.* (1976) and Boles and Franks (1979). It is unique and is restricted to 'closed' or 'nearly closed' argillaceous systems.

EXPERIMENTAL

Samples

The samples used in this study were provided by John Hower as representative of critical stages of the smectite-to-illite reaction sequence. They are shale cuttings from three depths (1750, 2450, and 5500 m) from a well (Case Western Reserve University Gulf Coast 6) drilled in Oligocene-Miocene Gulf Coast sediments. On the basis of XRD data, Hower *et al.* (1976) reported the mixed-layer I/S in these samples to contain approximately 20, 40, and 80% illite layers, respectively.

Methods

Samples for electron microscopic examination were prepared using the methods reported by Ahn and Peacor (1985a) and Lee *et al.* (1984). X-ray powder diffraction showed that the mineralogy of these samples was the same as that reported by Hower *et al.* (1976). Ion-thinned samples from thin sections were prepared following optical petrographic examination such that: (1) the thin section plane was normal to bedding so that (001) of phyllosilicates was preferentially parallel to the electron beam, and (2) the original textural relations within individual grains and between grains were preserved, i.e., the specimen preparation process introduced no artifacts that could be detected.

Specimens were examined at 100 kV in a JEOL JEM-100 CX scanning-transmission electron microscope (STEM) fitted with a solid-state detector for X-ray analysis. The resolving power for analytical electron microscopy (AEM) is about 300 Å. Thin edges were analyzed quantitatively following the procedures of Cliff and Lorimer (1975) and Lorimer and Cliff (1976). Standard minerals used to obtain proportionality constants ("k" values) for each element relative to Si were clinochlore for Mg, fayalite for Fe, adularia for K and Al, and plagioclase (Ab_{50}) for Na. Both standard minerals and shale specimens were analyzed at the same instrumental conditions in STEM mode and during the same observation sequence. Lattice fringe images were obtained using only 00*l* reflections and interpreted following Iijima and Buseck (1978).

The electron micrographs shown in Figures 1–13 are selected from hundreds of TEM images to illustrate commonly observed features. Because TEM images represent such small volumes, it is important to recognize that the samples studied here are representative of the full range of samples studied by Hower *et al.* (1976), that their mineral content was verified by standard X-ray diffraction and petrographic techniques, and that voluminous TEM results are in turn consistent with the same minerals in the same proportions.

TEM-AEM CHARACTERIZATION OF SMECTITE AND ILLITE

A problem exists in the characterization of smectite using lattice fringe images in that the vacuum of the TEM environment and/or direct irradiation by the electron beam may cause dehydration and collapse of smectite. If smectite does not collapse, it may be identified on the basis of its lattice fringe spacing of >10 Å. Collapse of the smectite structure, however, gives rise to an interlayer spacing of about 10 Å, a value also characteristic of illite.

Yoshida (1973) tried to characterize smectite using TEM by first expanding it with laurylamine hydrochloride. Unpublished studies of J. H. Lee and D. R. Peacor in this laboratory using Wyoming bentonite have shown that although laurylamine hydrochloride does indeed expand the layers of smectite, the effect is variable and some layers are hardly affected insofar as their lattice fringe images are concerned. Thus, the laurylamine hydrochloride treatment does not unambiguously distinguish between illite and smectite. An additional critical problem in using expanding reagents is that the original texture of the rock sample is destroyed. Treating a sample with laurylamine hydrochloride, for example, causes the expanded clay to spall.

Page and Wenk (1979) found that the lattice fringes of an untreated smectite displayed a 12–14-Å spacing that did not collapse in the TEM environment. Unpublished TEM experiments in this laboratory by J. H. Lee and D. R. Peacor of a Wyoming bentonite found an average basal spacing of 12 Å, similar to the value obtained by XRD on an untreated sample. On the other hand, Eggleton (1984) reported untreated smectite (saponite) displaying 10-Å lattice fringes, and concluded that smectite could not be distinguished from mica on the basis of lattice fringe images alone.

In the present study of unexpanded samples two distinct types of 10-Å layers have been repeatedly observed in all samples. One consisted of imperfect and curved layers having a 10–13-Å interlayer spacing, and the other consisted of straight, well-defined, relatively defect-free 10-Å layers. The former was abundant in shallower samples, whereas the latter became the dominant phase with increasing depth. The wavy layers having a 10–13-Å interlayer spacing were interpreted as smectite, and the straight layers were interpreted as illite based on textural and chemical data as shown in the following paragraphs. Characterization of these distinct types of layers as discrete smectite and illite is consistent with the trend showing a gradual increase of straight 10-Å layers and a gradual decrease of wavy 10-Å layers with increasing depth, parallel to the increase of illite with depth reported by Hower *et al.* (1976).

Two kinds of illite were observed in this study. Especially in samples from shallow depths one kind of illite was observed which had unique characteristics, including: (1) a layer stack-

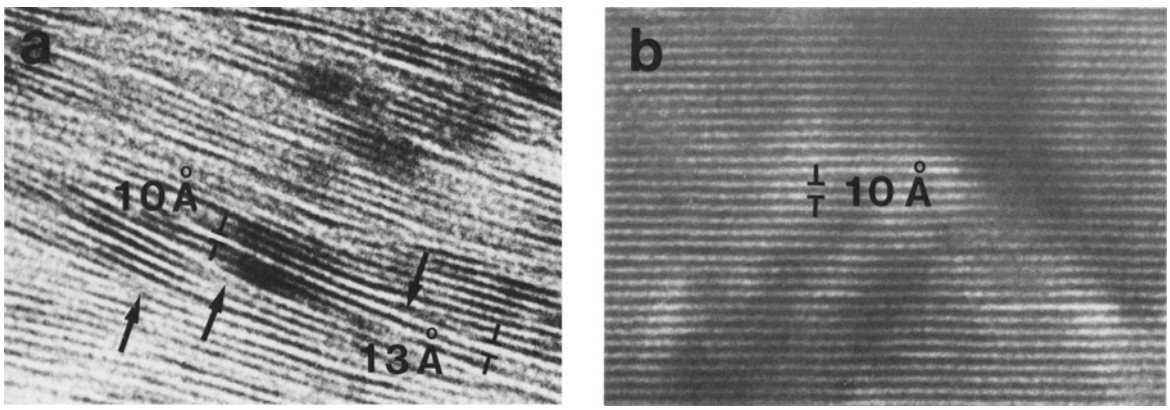

Figure 1. Typical lattice fringe images of (a) smectite from the 1750-m depth sample and (b) illite from the 5500-m depth sample. Smectite layers show many edge dislocations as indicated by arrows, and layer width varies along layers from 10 to 13 Å.

ing sequence corresponding to a two-layer polytype as observed in lattice fringe images and in electron diffraction patterns, (2) large grain size, in some samples exceeding 1 μm, and (3) bent layers having frayed and irregular surfaces, wherein layers terminated laterally at grain boundaries. Illite with these characteristics was probably detrital in origin, consistent with the significant amounts of detrital illite that are known to be present in Gulf Coast sediments (Hower, 1981). All results described below refer to illite which has entirely different characteristics.

Figure 1a shows typical lattice fringe images of 10-Å layers which were characterized as untreated smectite in the 1750-m depth sample. Lee *et al.* (1985) described the textural characteristics of both smectite and illite in these samples; hence, textural aspects of both minerals are only briefly described here. Individual layers of smectite are continuously curved with a general wavy appearance. Some lattice fringe spacings are as large as 13 Å but vary continuously along curving layers; most layers approach 10 Å in spacing and therefore presumably have collapsed subsequent to H_2O loss. The local variation in layer width may be related to local variation in chemistry and/or structure, but such differences cannot be determined with the data in hand. In addition, smectite layers commonly exhibit layer terminations (Figure 1a). Clusters of subparallel layers are generally thin and discontinuous, and the contrast varies from dark to light over short distances in an individual fringe.

Lattice fringe images of straight 10-Å layers, which were identified as illite, have features which are very different from those of smectite (Figure 1b). Layers appear as straight lattice fringes with constant 10-Å interlayer spacings. Layer terminations are relatively rare, and individual fringes are continuous and straight over considerable lengths as compared with smectite. In addition, image contrast is relatively unchanged along an individual fringe compared with smectite fringes, although packets of layers exhibit the "mottled" contrast that is characteristic of illite. As shown by Lee *et al.* (1984), the more homogeneous and defect-free illite is itself relatively imperfect in structure relative to micas which are characteristic of more advanced diagenesis.

Electron diffraction (ED) patterns of smectite and illite were found to be characteristically different in that 00*l* reflections of smectite were weak and diffuse parallel to c*. The average spacing of 001, however, was 10 Å, due presumably to collapse of layers. The weak reflections in the ED pattern of smectite (Figure 2a) reflect a lack of translational periodicity, as shown in lattice fringe images. The diffuseness along c* is primarily a reflection of the variable thickness of layers as shown in Figure 1a. Reflections are also diffuse normal to c* due to the curving of individual layers and the non-parallel orientation of adjacent layers (Figure 1a).

On the other hand, ED patterns of illite (Figure 2b) are characterized by relatively sharp, intense reflections, the sharpness and intensity being a function of the relative perfection of lattice fringes as shown in Figure 1b. ED patterns, however, cannot unambiguously be used to distinguish illite from smectite if the smectite layers have collapsed. If illite and smectite layers are intergrown (generally as packets of illite layers within subparallel smectite layers), the composite ED pattern is ambiguous; if the proportion of smectite layers is low, the reflections from smectite are so weak and diffuse that they are lost in the background.

Those imperfect layers which were shown be be smectite are rapidly damaged by the electron beam relative to illite layers. Lattice fringe images of smectite disappear within a few seconds when irradiated by a relatively intense electron beam. The instability of smectite under the electron beam relative to illite may be due to the presence (and subsequent release) of water and Na in interlayer sites of smectite (see Ahn *et al.*, 1985).

A final and more definitive method of characterization of smectite and illite is by means of AEM analyses which reflect the chemical differences between the two minerals. These data are described in detail below; however, smectite typically exhibits a high Si:Al ratio compared to illite, and low concentrations of both K and Na are usually detected as interlayer cations (Figure 3a). On the other hand, illite has a characteristically high K content and a higher Al:Si ratio than smectite (Figure 3b).

MICROSTRUCTURE OF SMECTITE AND ILLITE

1750-m depth sample

Figure 4 is a low-magnification TEM image showing the typical texture of clay minerals and non-phyllosilicates. The clay mineral in this image is almost entirely smectite with 001 lattice fringes perpendicular to the plane of the image. The anastomosing lattice fringe images of smectite typically exhibit changes in image contrast along layers, and some regions show no layers at all. Where contrast exists, but lattice fringes cannot

https://doi.org/10.1346/CCMN.1986.0340207 Published online by Cambridge University Press

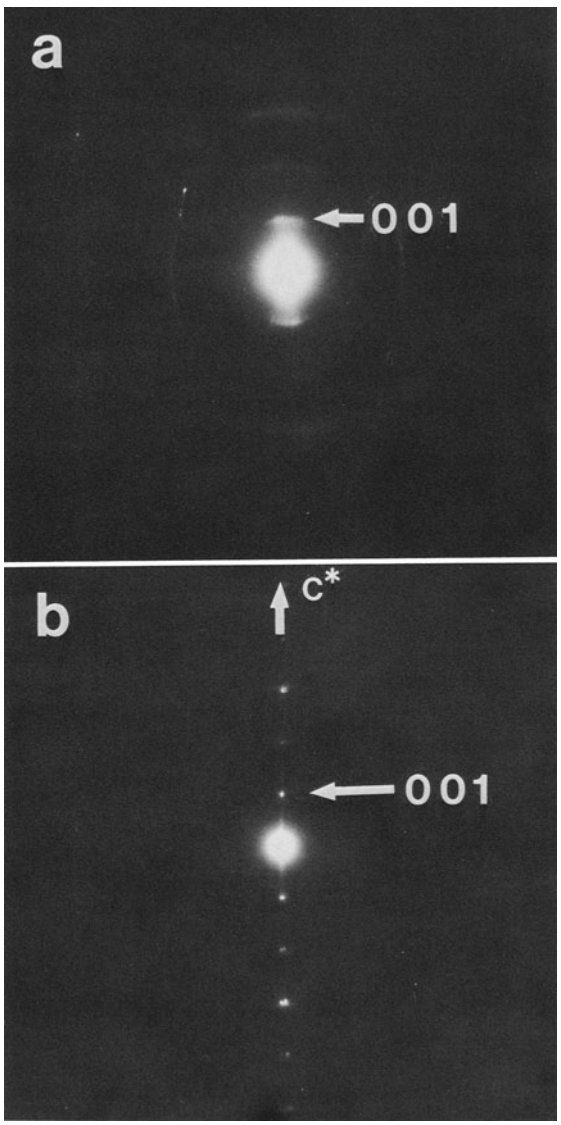

Figure 2. Typical electron diffraction patterns of (a) smectite and (b) illite. Reflections from smectite are very weak and diffuse compared to those of illite.

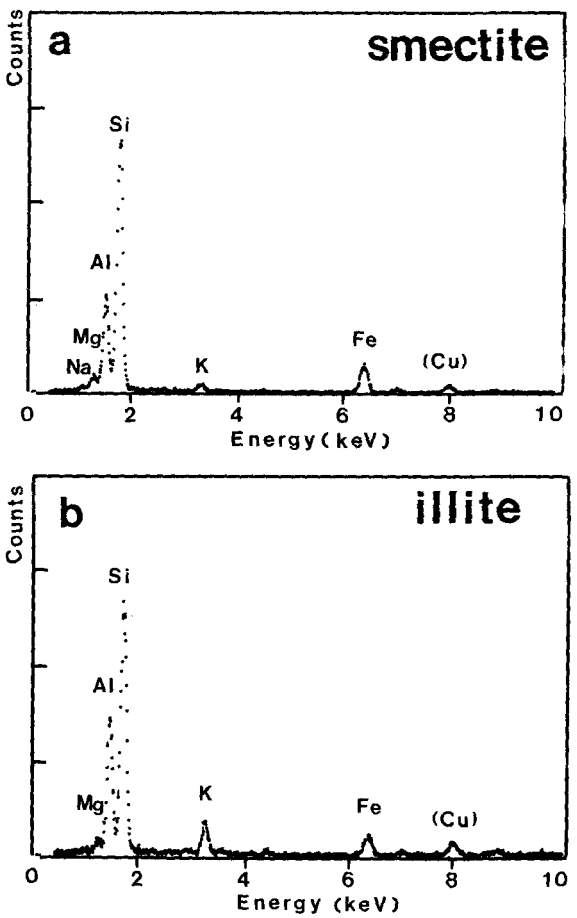

Figure 3. Energy dispersive X-ray spectra of typical (a) smectite and (b) illite. Al/Si ratio and K and Na concentrations are distinctly different in smectite and illite. Small Cu peaks in both spectra are due to contamination in the microscope.

be seen, smectite is usually present but oriented such that layers are not parallel to the electron beam. Even small rotations of the specimen relative to the beam direction give rise to large changes in contrast.

The overall state of imperfection that characterizes smectite in the early stages of diagenesis is clearly shown in Figure 4. Although layer orientations differ widely, the structures appear to be nearly continuous from point to point; i.e., even though individual layers may be only about 100 Å long in cross-section, continuous paths through coherent structural units can be traced from fringe to fringe and along fringes. The entire assemblage shown in Figure 4 thus appears to be a highly imperfect crystal; in effect, there is no grain boundary *per se,* as might be defined by an interface between separate smectite crystals. Only where smectite abuts against non-phyllosilicates can a boundary be observed. The term "megacrystal" is used here to describe such a continuous crystalline array. Smectite layers are subparallel to adjacent non-phyllosilicate grains and wrap around them. The curvature appears to be derived by compaction of the smectite around competent non-phyllosilicate grains. Clusters of imperfect packets of smectite layers have a characteristic lens-like shape. The term "grain," with its implications of well-defined surface area and continuous, well-defined periodic structure, has little relevance to the smectite described here.

2450-m depth sample

The 40% illite layers in the I/S of the 2450-m depth sample reflect an increase in the illite and decrease in the smectite content due to the transition of smectite to illite (Hower *et al.,* 1976). Illite occurs primarily as

https://doi.org/10.1346/CCMN.1986.0340207 Published online by Cambridge University Press

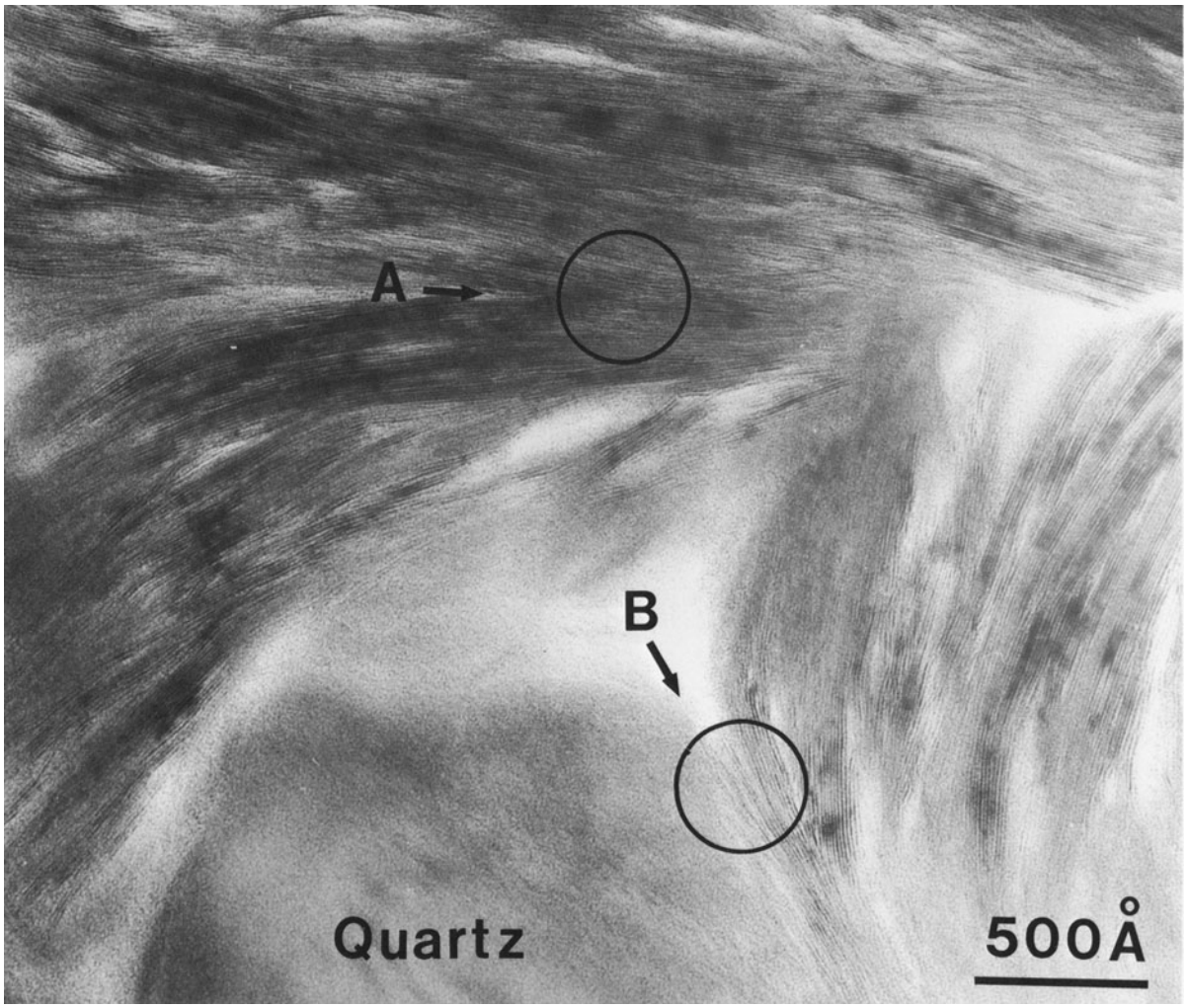

Figure 4. Low-magnification transmission electron microscope image from the 1750-m depth sample showing typical texture of smectite "megacrystal." Two clusters of smectite layers have coalesced (area A), and curving smectite layers conform to shape of quartz grain (area B).

50–100 Å thick packets of layers within smectite. As discussed above, smectite layers appear as imperfect and wavy fringes, whereas illite layers occur as packets of straight, relatively defect-free 10-Å layers (Figure 5a). Illite layers are parallel to the surrounding smectite layers but are locally only subparallel and are characterized by low-angle grain-boundary-like features; i.e., the fringes of one packet terminate along outer layers of an adjacent packet (Figure 5a). Illite packets, however, are rarely oriented at high angles to one another (Figure 5b).

The right-hand circle in Figure 5a illustrates one of the most common and significant textural relations noted in these samples. It includes a boundary between parallel layers of illite and subparallel layers of smectite. With few exceptions, the boundary between illite and smectite in the c* direction can be discerned. On the other hand, the relations between individual illite and smectite layers as imaged along layers in a direction normal to c* are difficult to observe. The left-hand circle in Figure 5a contains an "along-layer" boundary between smectite and illite. Lattice fringes of smectite and illite do not match each other at the boundary. Taking due consideration of the fact that lattice fringe images do not reflect detailed structure relations, we infer that the layers are not continuous across the "along-layer" interfaces. Boundaries normal to c* therefore separate discrete packets of illite layers from well-defined smectite, and individual fringes appear to be discontinuous across the "along-layer" boundaries.

Although packets of illite layers almost invariably were noted within smectite areas in the 2450-m depth samples, unaltered smectite was noted locally as discrete units. Figure 6 shows two distinct types of smec-

https://doi.org/10.1346/CCMN.1986.0340207 Published online by Cambridge University Press

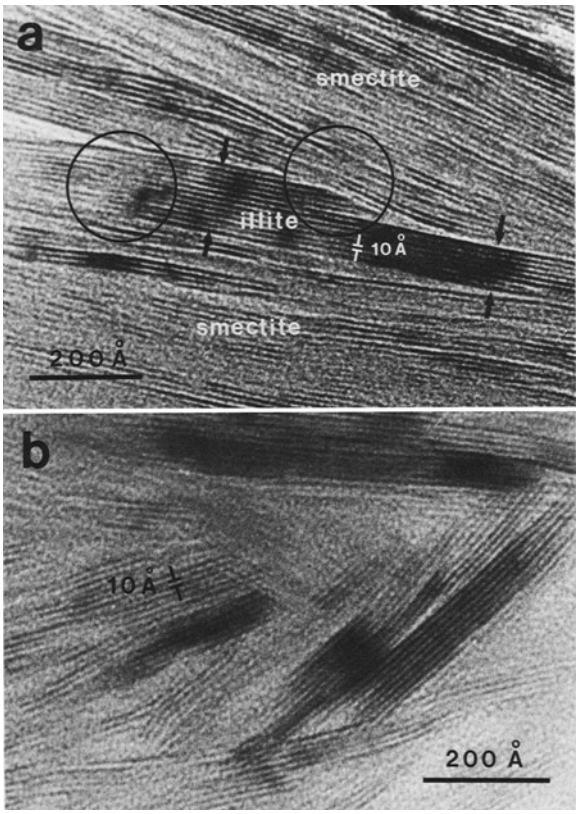

Figure 5. (a) Lattice fringe image from the 2450-m depth sample showing thin illite packet growing within subparallel smectite layers. Illite layers are not continuous with smectite layers along layer direction as shown in both circles. (b) Thin packets of illite layers oriented at large angles to one another.

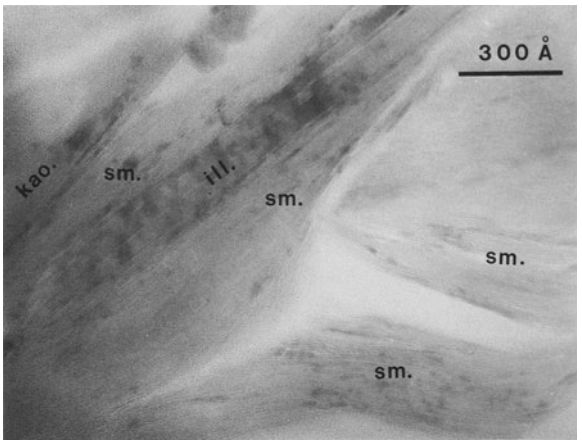

Figure 6. Low-magnification lattice fringe image from the 2450-m depth sample showing illite (ill.), smectite (sm.), and kaolinite (kao.) coexisting in the 2450-m depth sample. Packet of illite layers exists as core within matrix of smectite layers.

tite: one area contains a thick packet of illite layers as a core, and the other area consists only of smectite. The illite clearly exhibits a replacement texture, in that the volume now occupied by illite appears to have been previously occupied by parallel or subparallel layers of smectite.

5500-m depth sample

Smectite is scarce in TEM images of the 5500-m depth samples, and illite is the dominant phase (Figure 7). Illite packets are wider and thicker than those in the shallower samples, apparently reflecting continuous growth with increasing depth. Low-angle, grain-boundarylike features are common (Figure 7). Packets of layers, within which defects are rare, intersect subparallel layers at the boundaries. Separate packets of illite appear to be relatively defect-free, but each has a slightly different orientation due to the variable orientation of clusters of precursor smectite layers. Where such units coalesce they should form low-angle grain boundaries; however, as shown in Figure 8a, illite packets only locally display typical high-angle grain boundaries, due, presumably, to locally large differences in orientation of parent smectite layers.

The low-angle, grain-boundarylike features may also be derived by the growth of single packets of illite layers as illite encompasses smectite having especially divergent domains. For example, in Figure 8b, illite layers that appear coherent are interrupted by edge dislocations that cause local curvature of layers. Which of the two mechanisms gives rise to defects between illite packets usually cannot be ascertained.

CHEMICAL COMPOSITION OF SMECTITE AND ILLITE

AEM analyses were made of areas of smectite and illite that were apparently homogeneous in texture over areas larger than about 300 Å in diameter (resolution of the AEM analyses) and that displayed the typical textural characteristics described above. All quantitative analytical data for smectite were obtained from the 1750-m depth sample; those for illite were obtained from the 5500-m depth samples, because packets of illite layers within smectite in the 2450-m depth sample and smectite areas in the 5500-m depth samples were smaller than the resolving power of the technique. The chemical formulae of smectite and illite have net negative charge deficiencies, but they are well within analytical errors and the errors generated by assumptions during the process of normalizing of the elemental ratios.

The values for Al and Si are distinctly different for smectite and illite, although data for both phases show considerable scatter (Figure 9a). The smectites appear to vary more widely in Al and Si than the illites. The more Al and less Si in illite compared with smectite suggests that the increase in net negative charge in the 2:1 layer in illite is attained largely by the substitution

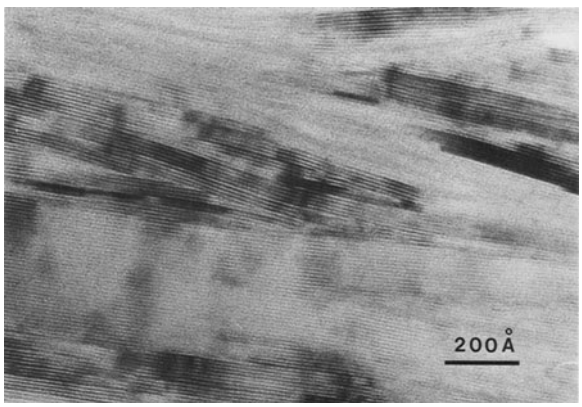

Figure 7. Lattice fringe image from the 5500-m depth sample. Thick packet of illite layers has apparently coalesced with adjacent subparallel thin packets of illite layers.

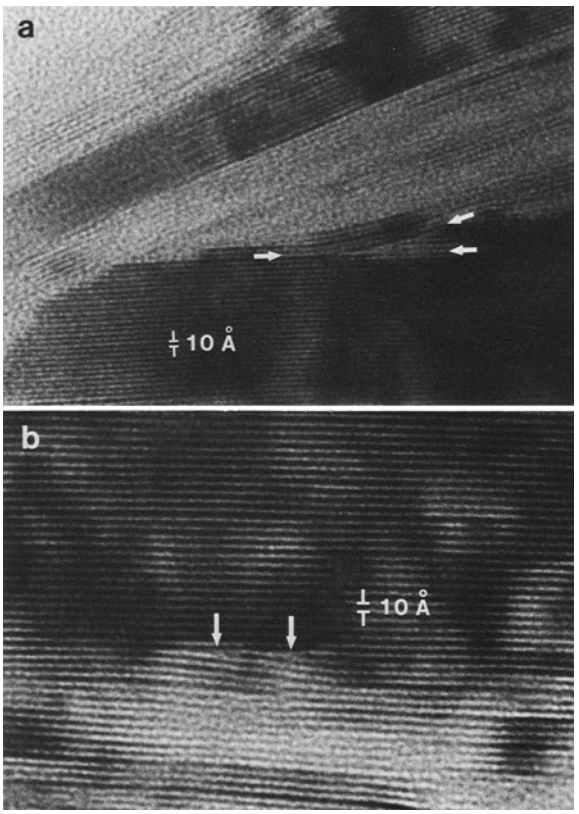

Figure 8. (a) Lattice fringe image from the 5500-m depth sample showing details of coalescing packets of illite layers. (b) Typical edge dislocations defined by terminations of layers of illite, possibly inherited from highly imperfect smectite structure (5500-m depth sample).

of Al for tetrahedrally coordinated Si (Perry and Hower, 1970; Hower *et al.,* 1976), although reduction of Fe may play an additional important role in increasing the net negative charge in 2:1 layers during the conversion process (Eslinger *et al.,* 1979).

The ranges of Fe and Mg in smectite are also greater than those in illite (Figures 9b and 9c). The Fe content of illite is significantly less than that of smectite, but the Mg content of the two phases is nearly the same. Thus, Fe appears to have been preferentially lost relative to Mg during the reaction. Hower *et al.* (1976) observed a decrease in Fe_2O_3 and MgO in clay concentrates in the same samples with increasing depth and increasing proportion of illite layers in I/S. Although the data were based on heterogeneous bulk samples, they agree with the AEM data presented here. In addition, Hower *et al.* (1976) suggested that the Fe and Mg released from smectite during its conversion to illite may have contributed to the formation of chlorite whose relative amount increased as the illite transformation proceeded. Ahn and Peacor (1985a) confirmed such a relation by a TEM and AEM study of the same samples described in the present paper. They noted that the chemical composition of chlorite and interstratified berthierine reflected the chemical changes that accompany the smectite-to-illite conversion; the high Fe content of chlorite relative to Mg is due to preferential loss of Fe relative to Mg. This reaction requires that not only Fe and Mg, but also components such as Al and Si, diffuse over distances at least as large as those separating illite, smectite, and chlorite; i.e., the Fe and Mg freed at the reaction interface must diffuse over distances of at least hundreds of Ångstroms.

Most smectites exhibited subequal proportions of Na and K as interlayer cations, but some were found to contain only Na or only K (Table 1). Smectite with $K \geq Na$ is the dominant variety. The presence of K in smectite is apparently not due to the presence of illite layers in the areas analyzed inasmuch as the negative charges of the 2:1 layers are within the range of negative charge of smectite. Significant amounts of K may be concentrated in smectite before smectite is converted to illite; data for cation-exchange free energies of K-for-Na in smectite (Tabikh *et al.,* 1960; Gast, 1969) indicate that K preferentially occupies interlayer sites in smectite, and that the preference for K increases very rapidly with decreasing P_{H_2O} (Tabikh *et al.,* 1960; Tardy *et al.,* 1985). Therefore, smectite may be enriched with K during deep burial even though pore solutions are richer in Na than K. In addition, if smectite is dehydrated, the selectivity of smectite for K becomes greater (Inoue and Minato, 1979; Inoue and Utada, 1983; Eberl, 1980). An increase in temperature and pressure during burial diagenesis may cause at least partial dehydration of some smectite layers and thus facilitate K-Na exchange. Although such reactions are problematical, these data strongly suggest that replacement of Na by K may take place prior to substitution of Al for Si. The K content of smectite may be due to

https://doi.org/10.1346/CCMN.1986.0340207 Published online by Cambridge University Press

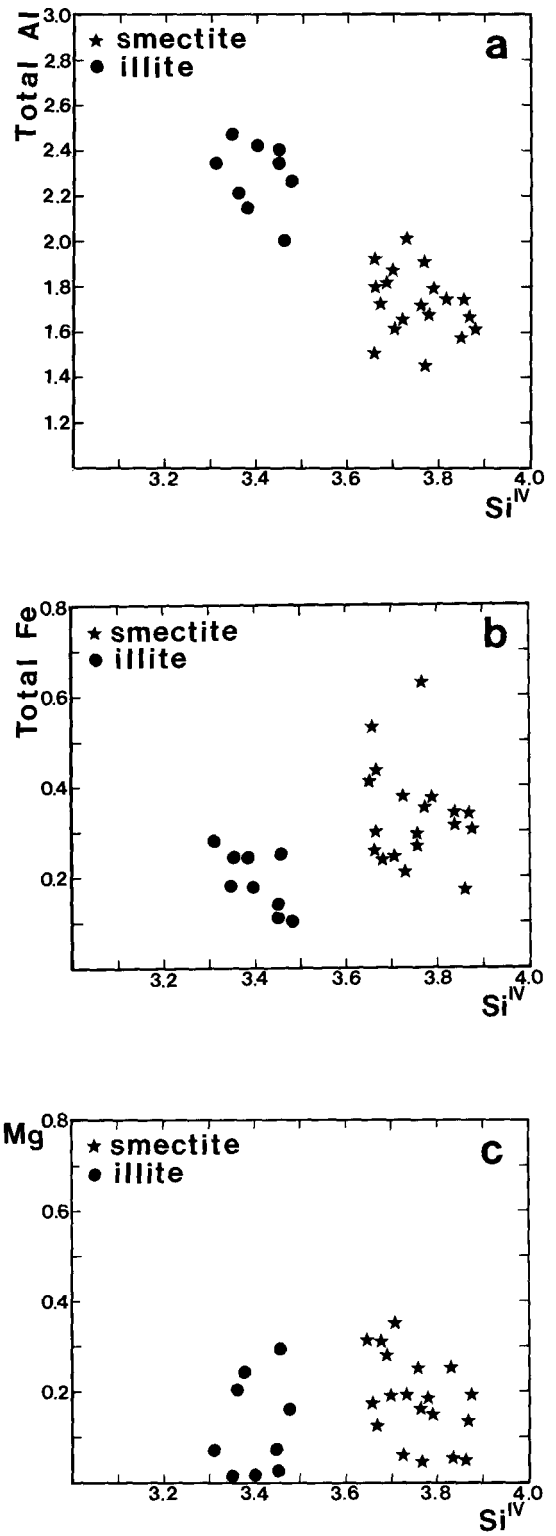

Figure 9. Plots of (a) total Al vs. Si, (b) Fe vs. Si, and (c) Mg vs. Si for smectite and illite as calculated for normalized analyses. Al and Fe contents are distinctly different, but Mg contents are similar for smectite and illite.

the presence of illite layers in the analyzed area; however, the low Al/Si ratio and low negative charge, as well as the low alkali contents as compatible with the low negative charge, indicate that analyzed areas are almost entirely smectite.

Although Ca is considered to be a common interlayer cation in smectite (see, Weaver and Pollard, 1973), Ca was not detected by AEM analysis. Significant amounts of Ca may be exchanged with Na in seawater during transportation (Sayles and Mangelsdorf, 1977, 1979); however, the chemical analyses of clay concentrates from the same samples show CaO contents greater even than those for Na_2O (Hower *et al.*, 1976). Thus, this Ca must be present in phases other than smectite, or samples for chemical analysis may have been affected by sample preparation (Sayles and Mangelsdorf, 1977).

The K, Al, and Si contents for illite vary only slightly compared with the broader ranges noted for smectite, presumably because detrital smectite formed in a variety of environments. The K-deficiency, Al-excess, and presence of Fe and Mg (relative to ideal muscovite) are similar to values obtained for illite of the Martinsburg shale by direct AEM analysis by Lee *et al.* (1984). The defects at interlayer sites, which correspond to about half of such sites, could potentially be occupied by H_3O^+. In addition, ammonium substitution for K, which cannot be detected by AEM analysis, could give rise to apparent low K contents in illite. Considerable ammonium has been reported to substitute for K in illite of Gulf Coast shales (Cooper and Abedin, 1981).

These quantitative data for smectite at AEM levels of resolution show that smectite is characterized by extreme heterogeneity in all components from grain to grain. The heterogeneity is so extreme as to imply that composition varies significantly even along single layers. Bulk chemical and analytical methods therefore yield average analyses of extremely heterogeneous smectites. Caution must therefore be used in interpreting the bulk chemistry of such clays especially those in shale which have been derived from diverse sources.

DISCUSSION

Smectite-to-illite reaction

TEM data show that in the 1750-m depth samples the dominant clay mineral smectite occurs as highly imperfect, discontinuous, anastomosing layers which collectively define a continuous structure (Figure 10). Illite occurs as thin packets of straight, relatively defect-free 10-Å layers within a matrix of smectite (Figure 11). The illite layers are parallel or subparallel to adjacent layers of smectite, but they are largely discontinuous in structure along the planes of layers as shown in Figures 5 and 11. With increasing depth, packets of illite layers thicken, become more abundant, and eventually coalesce as smectite is consumed. The final product is a continuous illite structure consisting of packets

https://doi.org/10.1346/CCMN.1986.0340207 Published online by Cambridge University Press

Table 1. Analytical electron microscopic analyses of smectite from the 1750-m depth sample. Cation ratios of smectite normalized to a total of 6 (IV + VI) cations.[1]

Elements[2,3]	1	2	3	4	5	6	7	8	9	10
K	0.17	0.00	0.12	0.17	0.32	0.07	0.24	0.32	0.05	0.14
Na	0.11	0.25	0.16	0.06	0.05	0.21	0.06	0.00	0.21	0.17
Si	3.88	3.73	3.70	3.73	3.87	3.86	3.76	3.66	3.67	3.84
Al(IV)	0.12	0.27	0.30	0.27	0.13	0.14	0.24	0.34	0.33	0.16
Al(VI)	1.50	1.74	1.57	1.38	1.53	1.60	1.47	1.16	1.39	1.41
Fe	0.31	0.21	0.24	0.43	0.34	0.35	0.28	0.53	0.30	0.34
Mg	0.19	0.05	0.19	0.19	0.13	0.05	0.25	0.31	0.31	0.25
Elements	11	12	13	14	15	16	17	18	19	Average
K	0.06	0.07	0.11	0.31	0.26	0.07	0.21	0.11	0.27	0.16
Na	0.18	0.21	0.18	0.02	0.12	0.18	0.06	0.24	0.02	0.13
Si	3.69	3.77	3.78	3.79	3.66	3.84	3.77	3.67	3.71	3.75
Al(IV)	0.31	0.23	0.22	0.21	0.34	0.16	0.23	0.33	0.29	0.25
Al(VI)	1.51	1.21	1.47	1.54	1.58	1.60	1.67	1.47	1.29	1.48
Fe	0.23	0.63	0.35	0.33	0.25	0.34	0.29	0.41	0.40	0.34
Mg	0.26	0.16	0.18	0.13	0.17	0.06	0.04	0.12	0.31	0.18

[1] Each column represents an analysis of an individual area.
[2] Mg and Al are assumed to be absent in interlayer sites of smectite.
[3] Fe includes total (Fe^{2+} + Fe^{3+}).

separated by small-angle grain boundaries where growing packets have come together (Figure 12). These interpretations suggest that illite formed by replacement of the original smectite in Gulf Coast sediments, and that the volume occupied by the product illite is the same as that previously occupied by smectite.

The data also suggest that the illite formation started in sites within smectite rather than at the boundaries of smectite (see Figure 11). These results are somewhat surprising in that the diffusion of chemical components through the grain to the transition sites might be expected to give rise to reaction at the edges of grains,

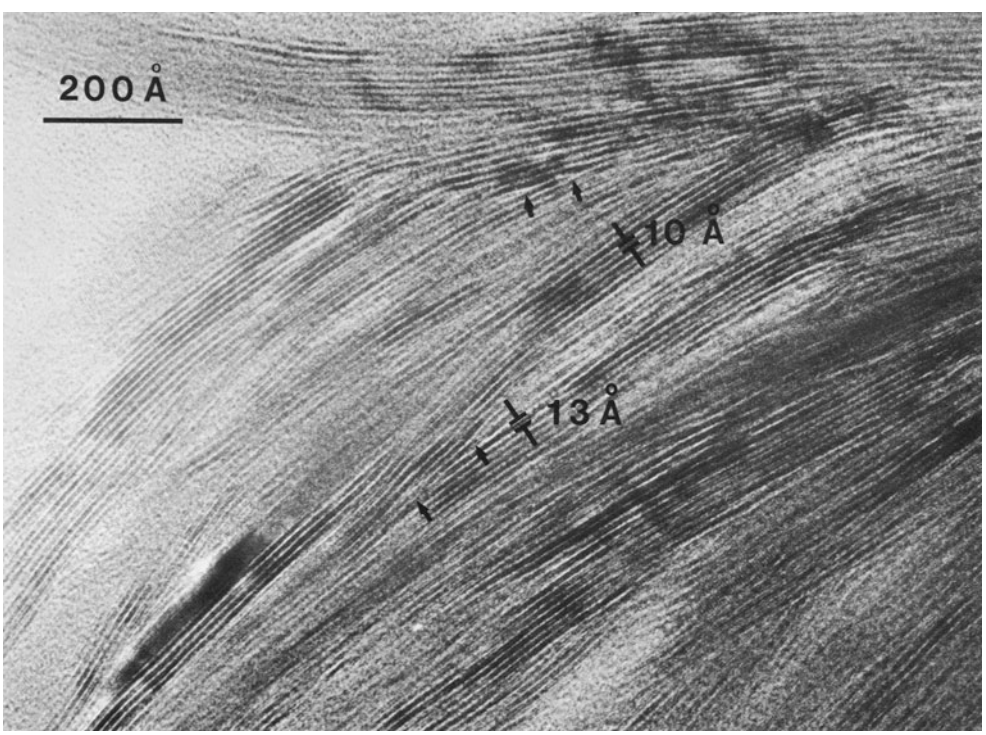

Figure 10. High-magnification lattice fringe image from the 1750-m depth sample showing typical discontinuous and wavy smectite layers having variable orientation. Edge dislocations are indicated by arrows.

https://doi.org/10.1346/CCMN.1986.0340207 Published online by Cambridge University Press

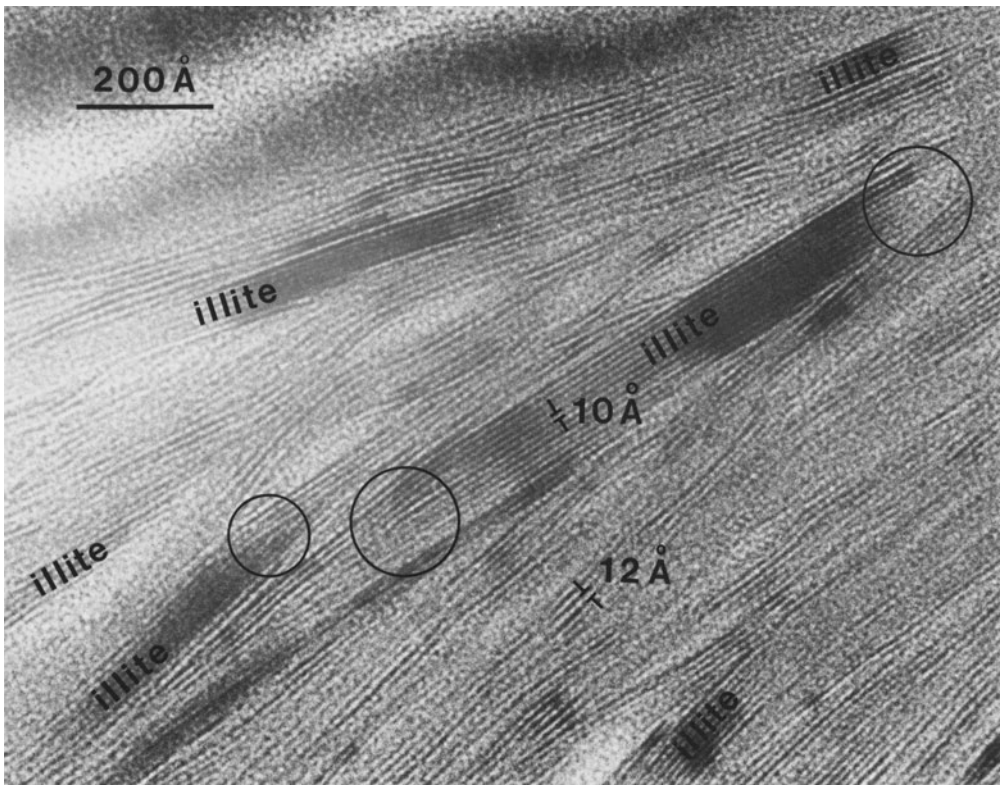

Figure 11. High-magnification lattice fringe image from the 2450-m depth sample. Illite occurs as 50–100-Å packets between subparallel smectite layers.

the usual situation, for example, in replacement reactions in prograde metamorphic rocks. The smectite is clearly heterogeneous in structure and chemistry, and thus it is possible that the embryonic illite layers may nucleate either at sites of unusually imperfect structure (e.g., dislocations which may also serve as diffusion pathways, see Veblen and Buseck, 1980; Veblen, 1985; Yau *et al.,* 1984) or where abnormally high original K and Al give rise locally to illite-like units within smectite.

Insofar as these data are able to show, the boundary between smectite and illite is discontinuous in chemistry, structure, and texture. Lattice fringes appear to be discontinuous along layers at smectite-illite boundaries, and illite occurs as discrete, well-defined packets within smectite, i.e., the structure is discontinuous at the boundaries between illite and smectite. The compositions of smectite and illite across the interface could not be determined directly because AEM cannot resolve such small areas; however, the AEM data for illite and smectite (Tables 1 and 2) from the 1750-m and 5500-m depth samples show that smectite and illite are chemically distinct. Such data collectively require that product illite be formed through considerable reconstitution of smectite in texture, structure, and chemistry. The transformation of smectite takes place across a reaction front such that the smectite structure is locally disrupted, i.e., as the transformation proceeds bonds within T-O-T layers of smectite are ruptured. Such a disarticulated state probably provides a ready path for the change in composition in both tetrahedral and octahedral sites which occurs on condensation of such structural units to add to the expanding illite packets.

It is well known among experimentalists in silicate systems that diffusion and interchange of Si and Al do not occur in the solid state at significant rates even at temperatures as high as 300°C. Inasmuch as the changes described above occurred at temperatures estimated to be <200°C (Hower *et al.,* 1976), and in part even <100°C, addition of Al, loss of Si and interchange of Al and Si could not reasonably have occurred in the solid state, i.e., without disruption of T-O-T units. Discontinuities in composition, structure, and texture at the smectite-illite interface thus require disruption, disarticulation, and reconstruction (at least in part) of T-O-T units. Such a relation is not only consistent with, but required by kinetic factors concerned with Al-Si interchange. Illite formation through the destruction of smectite is also consistent with oxygen isotope compositions of the same samples by Yeh and Savin (1977) who showed that the fine clay fraction (<0.1 μm) comes

https://doi.org/10.1346/CCMN.1986.0340207 Published online by Cambridge University Press

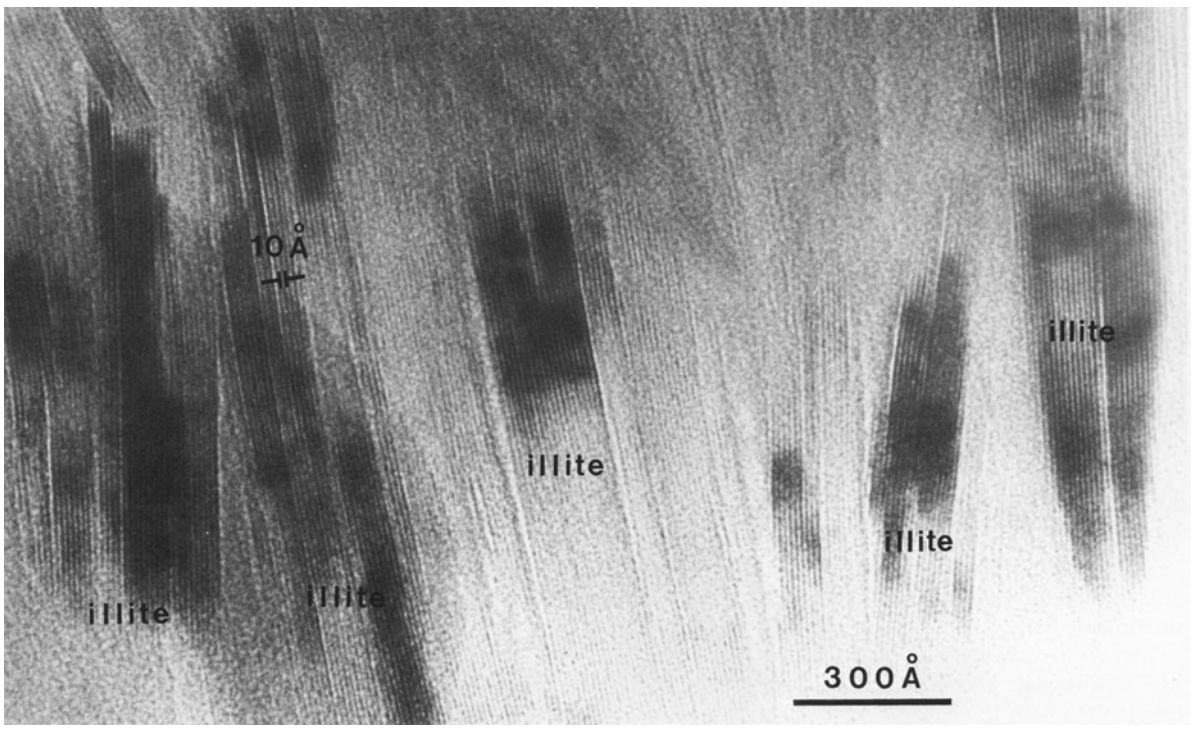

Figure 12. Abundant, thick, subparallel illite packets locally coalesced in the 5500-m depth sample.

to more complete oxygen isotope equilibrium with pore water with increasing burial depth and with increasing illite content. Disruption of the structure does not require that all the cation-anion bonds of smectite be broken; on the contrary, major subunits of structure (such as combinations of edge-sharing octahedra or condensed tetrahedral units) may retain their integrity during the transition.

The transformation involves almost a complete loss of Na as the principal interlayer cation in smectite and gain of K. For these cations, the source of K and the disposition of Na must be external to the smectite matrix. The significant K content of untransformed smectite containing the high Si:Al ratios characteristic of smectite are particularly informative. Significant K from external sources (e.g., K-feldspar and/or mica) may replace Na in smectite prior to illite conversion. Thus, the reaction may occur in two steps, the first of which involves at least partial exchange of K and Na, without disruption of T-O-T units, and with the production of K-smectite. Some K in smectite may exist as non-exchangable K (Inoue, 1983). The rate-determining step therefore must be the more sluggish Al-Si diffusion and local reconversion of T-O-T units at the transformation interface relative to the lower activation energy required for alkali cation exchange.

Given that significant gain or loss of components must occur, it remains to determine the pathway for diffusion through smectite. Veblen and Buseck (1980) pointed out that large tunnels parallel the layer termination direction in chain and sheet silicates and that "ultra" fast interstitial diffusion is possible through such tunnels. Yau *et al.* (1984) similarly noted that layer terminations provide dislocations several Ångstroms in diameter, which may serve as conduits for water and reactant and product ions. Smectite characteristically has a high density of layer terminations. They are so abundant as to destroy the sense of translation periodicity. The termination of a smectite layer, around which adjacent layers are distorted, must produce a channel about 10 Å in diameter. This size channel is more than adequate to serve as a conduit for cations or cation-(H_2O, OH^-) complexes. In any event, the imperfections in smectite apparently provide a ready pathway for the fast diffusion of cations and H_2O at the low temperatures required by the proposed transformation mechanism.

Mixed-layer illite/smectite: disagreement of XRD and TEM data

The observation from TEM data that packet thickness and abundance of illite both increase with depth is compatible with the trend determined by Hower *et al.* (1976) using XRD data, although the XRD data implied that the illite and smectite are present primarily as a mixed-layer phase based on the interpretation of calculated XRD patterns of Reynolds and Hower (1970). The TEM data reported here suggest

https://doi.org/10.1346/CCMN.1986.0340207 Published online by Cambridge University Press

Table 2. Analytical electron microscopic analyses of illite from the 5500-m depth sample. Cation ratios of illite normalized to a total of 6 (IV + VI) cations.[1]

Elements[2]	1	2	3	4	5	6	7	8	9	Average
K	0.64	0.72	0.56	0.63	0.52	0.66	0.62	0.68	0.61	0.63
Na	0.00	0.00	0.00	0.00	0.05	0.00	0.06	0.00	0.00	0.01
Si	3.45	3.48	3.38	3.45	3.46	3.35	3.31	3.36	3.40	3.40
Al(IV)	0.55	0.52	0.62	0.55	0.54	0.65	0.69	0.64	0.60	0.60
Al(VI)	1.85	1.74	1.52	1.80	1.46	1.82	1.65	1.56	1.82	1.69
Fe	0.13	0.10	0.24	0.13	0.25	0.18	0.28	0.24	0.18	0.19
Mg	0.02	0.16	0.24	0.07	0.29	0.00	0.07	0.20	0.00	0.12

[1] Each column represents an analysis of an individual area.
[2] Fe includes total (Fe^{2+} + Fe^{3+}).

that illite exists principally as packets of layers rather than as mixed-layer I/S. The transformation model presented here does not require a mixed-layer phase; rather it is based on the observation of separate domains of illite and smectite. Because the XRD and TEM data are in apparent conflict and because the nature of the smectite-illite intergrowth is central to any transition model, some additional discussion is warranted.

The AEM data (Tables 1 and 2) for the areas that can be texturally characterized as illite or smectite are compatible with the end-member phase so identified. Illite-free domains of smectite layers have been observed adjacent to thick packets of illite layers (which, in turn, appear to be devoid of smectite layers). The XRD data for the 5500-m depth sample imply that illite and smectite are present as an ordered mixed-layer phase, but TEM data show that illite is present as homogeneous packets 10 to 30 layers thick within a matrix of smectite. Although it is difficult to determine the ratios of layers of illite to smectite accurately, they appear to be present in an approximate ratio of 4:1 (I:S). Furthermore, AEM data for areas containing separate domains of both illite and smectite yield compositions which are intermediate between those of the end-member phases, but to the degree that is predicted by weighted analyses of the end-members on the basis of the approximate ratios of areas of the separate phases. Although the AEM and TEM data do not preclude the existence of some mixed-layer I/S in these samples, they do imply that the majority of illite or smectite is present as separate packets of subparallel layers.

Nadeau *et al.* (1984a, 1984b) suggested that clays which give XRD patterns of ordered mixed-layer phases are composed of aggregates of thin 'particles' whose surfaces behave similarly to the interlayer sites of smectite; i.e., they are capable of adsorbing water and organic molecules. Regularly interstratified mixed-layer I/S was thus described as consisting of thin 'illite' particles, two layers thick, and pure smectite as consisting of single unit layers, 10 Å thick. Our TEM observations of original unfractured shale samples, however, show that illite packets are usually thicker than 5 layers in the 2450-m depth sample which gave an XRD pattern of randomly interstratified I/S containing 40% illite layers, and thicker than 10 layers in the 5500-m depth sample which gave an XRD pattern of ordered I/S containing 80% illite layers. The discrepancy in the thickness of illite between our direct TEM observation and the indirect TEM observation of Nadeau *et al.* (1984a) may be due to different sample preparation methods; i.e., our data are based on unsegregated original shale samples and those of Nadeau *et al.* (1984a) are based on size-fractionated samples (<0.1 μm) prepared in the same way as for XRD study. Thus, the original packets of illite and smectite may have disarticulated to thinner units even down to a thickness of one or two layers as shown by Nadeau *et al.* (1984a, 1984b); such units were then presumably rearranged during specimen preparation for XRD examination. The direct observation of undisturbed textural relations by TEM and AEM methods, wherein illite and smectite are shown to be discrete phases, is thus a more accurate representation of the true state of illite and smectite in undisturbed samples. On the other hand, XRD patterns of disarticulated-reconstituted samples may have characteristics that reflect only the ratios of illite to smectite; thus the interlayer stacking relations are artifacts.

General geologic relations

The data described above have implications to the general relations surrounding the smectite-to-illite reaction. Central to these is the question of whether or not smectite and/or illite are thermodynamically stable phases. Lippman (1982), for example, concluded that illite, smectite, and most other clay minerals are "metastable or even completely unstable." In the Gulf Coast sediments described here, smectite and illite coexist in direct contact, as individual phases, over a considerable range of temperature. Quantitative chemical data are not available for all depths (temperatures), but qualitative data suggest that the composition of each phase does not vary. These relations suggest that smectite + illite cannot be an equilibrium assemblage inasmuch as smectite is reacting to yield illite over the range of depths. In addition, both smectite and illite, but especially smectite, are characterized by extreme

heterogeneity within a given sample. Variable composition both within and between domains of a given phase at a scale of hundreds of Ångstroms, the presence of high densities of imperfections such as edge-dislocations, and the existence of complex layer stacking relations are all consistent with metastability of the phases in which they occur. Indeed, Lee *et al.* (1985) pointed out how such heterogeneities decrease in extent as diagenetic grade increases. Because phases are heterogeneous does not prove that the defect-free equivalent phases are unstable; however, the observed heterogeneity is consistent with that relation.

Because at least one of the two phases is apparently thermodynamically unstable, and because they both exist over a range of temperatures and other conditions in a variety of geologic systems, the degree of reaction of smectite to illite must be controlled by kinetic factors (Eberl and Hower, 1976, 1977; Lahann and Roberson, 1980), i.e., temperature, time, activities of chemical components, and rock/water ratio must all significantly affect reaction rates. In a sequence wherein all other variables affecting reaction rates are constant, temperature may indeed be the principal factor affecting the smectite-to-illite ratio. Temperature is apparently the most important factor, at least to a first approximation, in the Gulf Coast sequence of sediments (Hower *et al.*, 1976). In other systems, however, different variables may be at least as important as temperature in controlling the smectite to illite ratio (e.g., Heling, 1978; Hoffman and Hower, 1979; Eslinger and Sellars, 1981). Extreme caution must therefore be used in applying the degree of conversion of smectite to illite in determining burial depth or temperature.

Closed vs. open system

Hower *et al.* (1976) concluded that argillaceous Gulf Coast sediments behaved essentially as a closed system for all components except H_2O, CaO, Na_2O, and CO_2. This conclusion was based, in part, on chemical analyses that showed the bulk chemistry of the sediments to be essentially constant even though significant mineralogical changes occurred with increasing depth. The Na and Ca content of these sediments, however, decreased with depth, and assuming that this decrease is due to a loss from the sediments (as opposed to a change in original sediment composition), the system should not be defined as "closed" in a true thermodynamic sense. Nevertheless, terms such as "nearly closed" are useful, and they are used here with the caveat that they are not used in a strict sense.

Gulf Coast shales are remarkable in that even at a depth of 5500 m presumably non-equilibrium assemblages of relatively reactive clay minerals exist. The coexistence of smectite and illite implies that factors controlling reaction rates have had only a minimal effect. Similarly, the abundance of structural imperfections show that these phases have persisted in a relatively high energy state compared to their defect-free equivalents. Because water is the principal medium for cation transport, these relations imply that these systems have not been affected by significant volumes of water, at least not since their initial compaction. The mechanism proposed for the transformation requires that water be present to act as a catalyst for local reconstruction of the structure at the reaction interfaces, and for ion transport over short distances; however, changes in texture require only locally very small amounts of water.

The significance of these relations is clear when they are compared with the observations of Yau *et al.* (1983) on Salton Sea sediments that are affected by actively convecting geothermal brines. In shallow sediments some smectite was replaced by illite in a manner duplicating the Gulf Coast reaction relations. In the same samples and in those from greater depth, however, euhedral illite laths were observed in open pore space. This illite, which predominates even at shallow depths, was described as having crystallized directly from solution. The necessary components were partly derived by dissolution of detrital smectite. Transport of dissolved components to distant sites then gave rise to direct crystallization of illite. Such an active geothermal system with a high relative water/rock ratio, high proportion of pore space, and active flow of saline solutions must have allowed local domains of shale to act as open systems. The smectite-to-illite reaction mechanism described in the present paper thus appears to be applicable to closed or nearly closed geological systems, at least as compared with the smectite solution-ion transport-illite crystallization mechanism occurring in the open Salton Sea system. Recognition that separate mechanisms exist for conversion of smectite to illite in different environments is a key factor in rationalizing conflicting data regarding the smectite-to-illite reaction.

Lastly, laboratory experiments in which smectite has been converted to illite generally require water to accelerate reaction rate (e.g., Eberl and Hower, 1977; Eberl, 1978a, 1978b). Such experiments must more nearly approximate open geologic systems in which dissolution of smectite yields components in solution that precipitate as illite at sites distant from the original smectite. Results from such experiments may not be directly applicable to the transition mechanism described here, where illite directly replaces smectite.

SUMMARY AND MODEL OF REACTION MECHANISM

The reaction of smectite to illite as implied by Hower *et al.* (1976) involves retention of the basic structure of 2:1 layers; only the chemistry of those units was envisioned as changing, with loss of Si, Na, and H_2O and gain in K and Al. On the other hand, Boles and Franks (1979) proposed an alternative mechanism

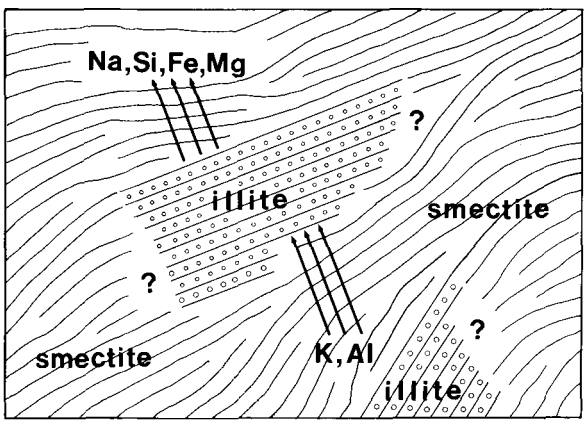

Figure 13. Schematic drawing illustrating principal features of model for transformation of smectite to illite in Gulf Coast argillaceous sediments.

which required destruction of some original smectite layers to provide necessary Al for illite formation. Our model for illite formation contrasts with these and others in large part because it is based on structural, chemical, and textural discontinuities at the interfaces between smectite and illite, and because smectite and illite are seen to be present as separate discrete domains rather than as a mixed-layer clay.

Figure 13 schematically shows the principal components of our model. Smectite is shown here as containing anastomosing layers with variable thickness and abundant dislocations and as forming continuous structural units referred to as "megacrystals." Packets of illite layers are present within the subparallel imperfect smectite matrix; however, layers of illite are well-defined, straight, and relatively defect-free compared with smectite layers. The boundaries between illite and smectite are parallel to c*, and layers of illite are discontinuous with layers of smectite in the "along-layer" direction. K and Al are shown diffusing through the smectite matrix to the transition boundary, and Na, Si, Fe, and Mg are shown diffusing away. The abundant defects in smectite probably serve as pathways for ion transport. K replacement of Na may precede illite formation and result in the formation of a K-smectite. The absolute amounts of Al gained or Si lost during the smectite-to-illite reaction depend on factors which cannot be assessed from the available data.

The transformation probably involves the breakdown of major parts of both octahedral and tetrahedral units, facilitated by the presence of H_2O, with change in composition of both tetrahedral and octahedral sheets occurring as a consequence of reconstruction of relatively defect-free 2:1 layers (illite). The reaction rate is thus largely dependent on such structural and chemical reconstruction. If K is not available, kaolinite may be produced (Eberl, 1971; Ahn and Peacor, 1985b). Fe and Mg diffuse to new sites, serving as the source for formation of chlorite interstratified with berthierine (Ahn and Peacor, 1985a).

Although not shown in Figure 13, as the reaction proceeds the boundaries of illite packets advance until they coalesce (Figures 7 and 12). Because illite inherits a layer orientation of the smectite where it nucleates (Figure 11), and because smectite layers are divergent (Figure 10), layers of illite packets will be subparallel where they intersect, resulting in small-angle grain-boundarylike features (Figure 12). The final texture will be dominated by thick illite packets with subparallel orientations.

ACKNOWLEDGMENTS

We are especially grateful to the late John Hower for providing us with his samples and data, for introducing D.R.P. to the world of clay minerals, and most of all for his encouragement and support, without which this research would not have been possible. We are thankful to E. J. Essene and B. H. Wilkinson for their valuable comments on early versions of the manuscript. We are also grateful to J. R. Boles, D. D. Eberl, F. A. Mumpton, R. C. Reynolds, Jr., and J. Środoń for their critical reviews and valuable suggestions. We thank W. C. Bigelow and the staff of the University of Michigan Electron Microbeam Laboratory for their help with respect to the STEM facilities and J. H. Lee and Y. C. Yau for their help and data. This study was supported by NSF grants EAR-8107529 and EAR-8313236 to D. R. Peacor.

REFERENCES

Ahn, J. H. and Peacor, D. R. (1985a) Transmission electron microscopic study of diagenetic chlorite in Gulf Coast argillaceous sediments: *Clays & Clay Minerals* **33,** 228–236.

Ahn, J. H. and Peacor, D. R. (1985b) The smectite to kaolinite transformation in Gulf Coast argillaceous sediments: a TEM and AEM study: in *Program and Abstracts International Clay Conference, Denver, Colorado, 1985,* p. 4.

Ahn, J. H., Peacor, D. R., and Essene, E. J. (1985) Coexisting paragonite-phengite in blueschist eclogite: a TEM study: *Amer. Mineral.* **70,** 1193–1204.

Aronson, J. L. and Hower, J. (1976) The mechanism of burial metamorphism of argillaceous sediments: 2. Radiogenic argon evidence: *Geol. Soc. Amer. Bull.* **87,** 738–744.

Boles, J. R. and Franks, S. G. (1979) Clay diagenesis in Wilcox sandstones of southeast Texas: implications of smectite diagenesis on sandstone cementation: *J. Sed. Petrol.* **49,** 55–70.

Burst, J. F. (1969) Diagenesis of Gulf Coast clayey sediments and its possible relation to petroleum migration: *Amer. Assoc. Petrol. Geol. Bull.* **53,** 73–93.

Cliff, G. and Lorimer, G. W. (1975) The quantitative analysis of thin specimens: *J. Microsc.* **103,** 203–207.

Cooper, J. E. and Abedin, K. Z. (1981) The relationship between fixed ammonium-nitrogen and potassium in clays from a deep well on the Texas Gulf Coast: *Texas J. Sci.* **33,** 103–111.

Eberl, D. D. (1971) Experimental diagenetic reactions involving clay minerals: Ph.D. thesis, Case Western Reserve Univ., Cleveland, Ohio, 145 pp.

Eberl, D. (1978a) The reaction of montmorillonite to mixed-layer clay: the effect of interlayer alkali and alkaline earth cations: *Geochim. Cosmochim. Acta* **42,** 1–7.

Eberl, D. (1978b) Reaction series for dioctahedral smectites: *Clays & Clay Minerals* **26,** 327–340.

Eberl, D. D. (1980) Alkali cation selectivity and fixation by clay minerals: *Clays & Clay Minerals* **28,** 161–172.

Eberl, D. D. (1984) Clay mineral formation and transportation in rocks and soils: *Phil. Trans. Roy. Soc. Lond.* **A311,** 241–259.

Eberl, D. and Hower, J. (1976) The kinetics of illite formation: *Bull. Geol. Soc. Amer.* **87,** 1326–1330.

Eberl, D. and Hower, J. (1977) The hydrothermal transformation of sodium and potassium smectite into mixed-layer clay: *Clays & Clay Minerals* **25,** 215–227.

Eggleton, R. A. (1984) Formation of iddingsite rims on olivine: a transmission electron microscope study: *Clays & Clay Minerals* **32,** 1–11.

Eslinger, E., Highsmith, P., Albers, D., and deMayo, B. (1979) Role of iron reduction in the conversion of smectite to illite in bentonites from the Disturbed Belt, Montana: *Clays & Clay Minerals* **27,** 327–338.

Eslinger, E. and Sellars, B. (1981) Evidence for the formation of illite from smectite during burial metamorphism in the Belt Supergroup, Clark Fork, Idaho: *J. Sed. Petrol.* **51,** 202–216.

Gast, R. G. (1969) Standard free energies of exchanges of alkali metal cations on Wyoming bentonite: *Soil Sci. Soc. Amer. Proc.* **33,** 37–41.

Heling, D. (1978) Diagenesis of illite in argillaceous sediments of the Rhinegraben: *Clay Miner.* **13,** 211–220.

Hoffman, J. and Hower, J. (1979) Clay mineral assemblages as low grade metamorphic geothermometers: application to the thrust faulted Disturbed Belt of Montana, U.S.A.: *Soc. Econ. Paleontol. Mineral. Spec. Publ.* **26,** 55–79.

Hower, J. (1981) Shale diagenesis: in *Clays and the Resource Geologist,* F. J. Longstaffe, ed., Short Course Handbook **7,** Mineral. Assoc. Canada, 60–80.

Hower, J., Eslinger, E. V., Hower, M. E., and Perry, E. A. (1976) Mechanism of burial metamorphism of argillaceous sediments: 1. Mineralogical and chemical evidence: *Geol. Soc. Amer. Bull.* **87,** 725–737.

Iijima, S. and Buseck, P. R. (1978) Experimental study of disordered mica structure by high-resolution electron microscopy: *Acta Crystallogr.* **A34,** 709–719.

Inoue, A. (1983) Potassium fixation by clay minerals during hydrothermal treatment: *Clays & Clay Minerals* **31,** 81–91.

Inoue, A. and Minato, H. (1979) Ca-K exchange reaction and interstratification in montmorillinite: *Clays & Clay Minerals* **27,** 393–401.

Inoue, A. and Utada, M. (1983) Further investigation of a conversion series of dioctahedral mica/smectite in the Shinzan hydrothermal alteration area, northeast Japan: *Clays & Clay Minerals* **31,** 401–412.

Lahann, R. W. and Roberson, H. E. (1980) Dissolution of silica from montmorillonite: effect of solution chemistry: *Geochim. Cosmochim. Acta* **44,** 1937–1943.

Lee, J. H., Ahn, J. H., and Peacor, D. R. (1985) Textures in layered silicates: progressive changes through diagenesis and low-temperature metamorphism: *J. Sed. Petrol.* **55,** 532–540.

Lee, J. H., Peacor, D. R., Lewis, D. D., and Wintsch, R. P. (1984) Chlorite-illite/muscovite interlayered and interstratified crystals: a TEM/STEM study: *Contrib. Mineral. Petrol.* **88,** 372–385.

Lipmann, F. (1982) The thermodynamic status of clay minerals: in *Proc. Int. Clay Conf., Bologna, Pavia, 1981,* H. van Olphen and F. Veniale, eds., Elsevier, Amsterdam, 475–485.

Lorimer, G. W. and Cliff, G. (1976) Analytical electron microscopy of minerals: in *Electron Microscopy in Mineralogy,* H. R. Wenk, ed., Springer, Berlin, 506–519.

Nadeau, P. H., Tait, J. M., McHardy, W. J., and Wilson, M. J. (1984a) Interstratified XRD characteristics of physical mixtures of elementary clay particles: *Clay Miner.* **19,** 67–76.

Nadeau, P. H., Wilson, M. J., McHardy, W. J., and Tait, J. M. (1984b) Interparticle diffraction: a new concept for interstratified clays: *Clay Miner.* **19,** 757–769.

Page, R. H. and Wenk, H. R. (1979) Phyllosilicate alteration of plagioclase studied by transmission electron microscopy: *Geology* **7,** 393–397.

Perry, E. and Hower, J. (1970) Burial diagenesis in Gulf Coast pelitic sediments: *Clays & Clay Minerals* **18,** 165–177.

Powers, M. C. (1967) Fluid-release mechanisms in compacting marine mudrocks and their importance in oil exploration: *Amer. Assoc. Petroleum Geol. Bull.* **51,** 1240–1254.

Reynolds, R. C., Jr. and Hower, J. (1970) The nature of interlayering in mixed-layer illite/montmorillonite: *Clays & Clay Minerals* **18,** 25–36.

Roberson, H. E. and Lahann, H. E. (1981) Smectite to illite conversion rates: effects of solution chemistry: *Clays & Clay Minerals* **29,** 129–135.

Sayles, F. L. and Mangelsdorf, P. C., Jr. (1977) The equilibration of clay minerals with seawater: exchange reactions: *Geochim. Cosmochim. Acta* **41,** 951–960.

Sayles, F. L. and Mangelsdorf, P. C., Jr. (1979) Cation-exchange characteristics of Amazon River suspended sediment and its reaction with seawater: *Geochim. Cosmochim. Acta* **43,** 767–779.

Środoń J. and Eberl, D. (1984) Illite: in *Micas, Reviews in Mineralogy, Vol. 13,* S. W. Bailey, ed., Mineralogical Society of America, Washington, D.C., 495–544.

Tabikh, A. A., Barshad, I., and Overstreet, R. (1960) Cation exchange hysteresis in clay minerals: *Soil Sci.* **90,** 219–226.

Tardy, Y., Duplay, J., and Fritz, B. (1985) The stability field of clay minerals as function of their composition and temperature of formation: in *Abstracts, 1985 International Clay Conference, Denver, Colorado,* p. 234.

Veblen, D. R. (1985) Extended defects and vacancy nonstoichiometry in rock-forming minerals: in *Point Defects in Minerals, Geophysical Monograph* **31,** R. N. Shock, ed., American Geophysical Union, Washington, D.C., 122–131.

Veblen, D. R. and Buseck, P. R. (1980) Microstructure and reaction mechanism in biopyriboles: *Amer. Mineral.* **65,** 599–623.

Weaver, C. E. and Beck, K. C. (1971) Clay-water diagenesis during burial: how mud becomes gneiss: *Geol. Soc. Amer. Spec. Pap.* **134,** 96 pp.

Weaver, C. E. and Pollard, L. D. (1973) *The Chemistry of Clay Minerals:* Elsevier, Amsterdam, 213 pp.

Yau, Y. C., Anovitz, L. M., Essene, E. J., and Peacor, D. R. (1984) Phlogopite-chlorite reaction mechanisms and physical conditions during retrograde reaction in the Marble Formation, Franklin, New Jersey: *Contrib. Mineral. Petrol.* **88,** 299–308.

Yau, Y. C., Lee, J. H., Peacor, D. R., and McDowell, S. D. (1983) TEM study of illite diagenesis in shale of Salton Sea geothermal field, California: in *Program and Abstracts, 20th Annual Meeting, Clay Minerals Society, Buffalo, New York, 1983,* p. 42.

Yeh, H.-S. and Savin, S. M. (1977) The mechanism of burial diagenetic reactions in argillaceous sediments: 3. Oxygen isotope evidence: *Bull. Geol. Soc. Amer.* **88,** 1321–1330.

Yoshida, T. (1973) Elementary layers in the interstratified clay minerals as revealed by electron microscopy: *Clays & Clay Minerals* **21,** 413–420.

(Received 18 January 1985; accepted 1 October 1985; Ms. 1445)